Received 21 December 2017; revised 14 January 2018; accepted 16 January 2018. Date of publication 5 February 2018;
date of current version 4 May 2018. The review of this paper was arranged by Editor M. Chan.

Digital Object Identifier 10.1109/JEDS.2018.2801278

Bipolar Resistive Switching Characteristics in Flexible Pt/MZT/Al Memory and Ni/NbO_2/Ni Selector Structure

KE-JING LEE, YU-CHI CHANG, CHENG-JUNG LEE, LI-WEN WANG, AND YEONG-HER WANG (Member, IEEE)

Institute of Microelectronics, Department of Electrical Engineering, National Cheng-Kung University, Tainan 701, Taiwan

CORRESPONDING AUTHOR: Y.-H. WANG (e-mail: yhw@ee.ncku.edu.tw)

This work was supported by the Ministry of Science and Technology of Taiwan under Contract NSC102-2221-E-006-182-MY3 and Contract MOST 105-2221-E-006-193-MY3.

ABSTRACT The use of a threshold-switching Ni/NbO_2/Ni device with a memory-switching Pt/magnesium zirconate titanate/Al device on a flexible substrate was proposed to suppress undesired sneak currents. The proposed flexible one selector and one resistor (1S1R) memory device exhibits a low operation voltage, good ON/OFF ratio of 10^5, uniform current distribution, excellent flexibility, and stable I–V curve at 85 °C. The good selection and memory properties of the flexible 1S1R memory device are highly promising for high-density and low-power flexible electronic applications.

INDEX TERMS Bipolar resistive switching, flexible, memory, selector, sol-gel.

I. INTRODUCTION

Resistive random access memory (RRAM) is one of the most promising candidates for next-generation nonvolatile memories given its simple structure, excellent scalability for flexible electronic applications, and high-density integration [1]–[3]. The flexible electronics has the potential to revolutionize portable inexpensive electronics. Flexible electronic devices are attractive candidates for next-generation display technology and are rapidly increasing in popularity all over the world. Given that a RRAM device has the problem of sneak-path currents through neighboring cells, this unintended current leakage paths must be eliminated. To settle the sneak-path issue, various categories have been proposed, such as the direct connection of another functional device to each RRAM cell [4], the construction of self-rectifying RRAM cells [5], or consists of two identical bipolar RRAM cells that are connected back-to-back by a common electrode [6], [7]. The direct connection of selector to each RRAM cell (1S1R) is one of the effective solutions for the sneak-path issue. The threshold-switching of a selector device forms a metallic-phase conductive filament as a result of local Joule-heating-induced insulator–metal transitions (I–M–T) of the corresponding sub-oxides [8]. Thus, the selection of suitable resistive and switching materials is an important step in the successful fabrication of a flexible 1S1R memory device [9], [10]. V, Nb, Ti, Ta, and Fe oxides exhibit threshold switching [11]. VO_2, a well-known threshold switching material, can function as a bidirectional switch [12]. Although connecting a VO_2-based threshold-switching device with a memory-switching device can address sneak path currents through neighboring cells, the operation temperature (∼67 °C) of VO_2 material is too low for the operation of the 1S1R memory device [13].

In term of the values of I–M–T temperature, the NbO_2 selector device has more potential to work at higher temperature compared with a VO_2 selector device [14]–[20]. The I–M–T temperature of NbO_2 is around 1080 K [21].

Furthermore, due to the stability is also an important issue for the flexible 1S1R memory device, the low temperature sol-gel magnesium zirconate titanate (MZT) thin film as the resistive layer of 1R was proposed. Zr^{4+} (ionic radius of 0.086 nm) are more chemically stable than Ti^{4+} (ionic radius of 0.075 nm) and have a large ionic size that can occupy the perovskite lattice [22]. The substitution of Ti by Zr depresses conduction by electronic hopping between Ti^{4+} and Ti^{3+}, thus decreasing the leakage current of the $BaTiO_3$ system. The principle of the MZT material is similar to that of BZT material, wherein improved resistive switching properties result from the substitution of Ti by Zr, which decreases the path of leakage current. The combination of a threshold-switching Ni/NbO_2/Ni device with a memory-switching Pt/MZT/Al device on flexible substrate

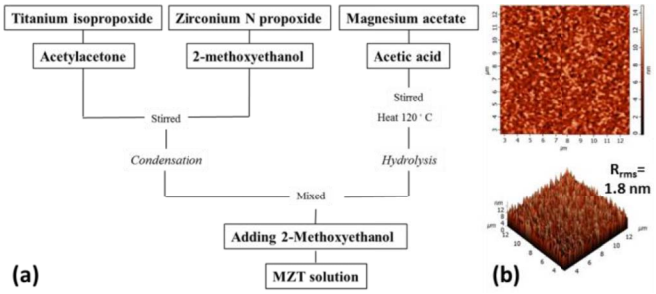

FIGURE 1. **(a) Flowchart for the preparation of MZT solution. (b) AFM images of the MZT thin film.**

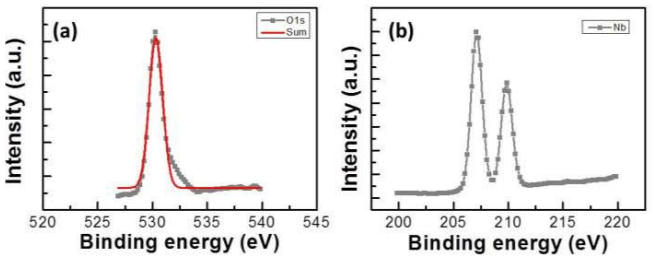

FIGURE 2. **XPS survey spectra of the NbO_2 thin film.**

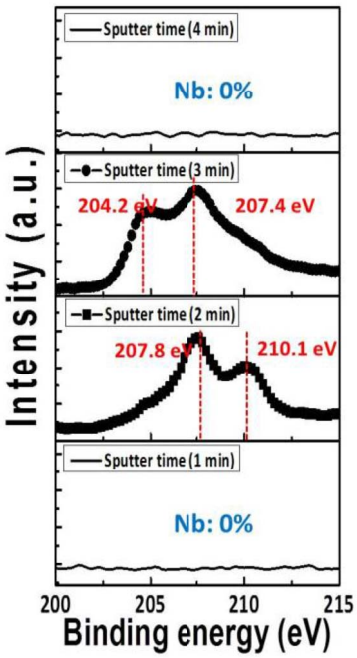

FIGURE 3. **Atomic concentration of Nb measured by the XPS depth profile in NbO_2-based MIM structure.**

is proposed in the present work. The proposed flexible 1S1R memory device exhibits a low threshold current, low operation voltage, good ON/OFF ratio of 10^5, uniform voltage/current distribution, excellent flexibility, and stable I–V curve at 85 °C.

II. DEVICE STRUCTURE AND FABRICATION

1S1R memory devices were fabricated on a low-cost flexible PET substrate. To fabricate the Ni/NbO_2/Ni selector, Ni electrodes and NbO_2 thin film were deposited by sputtering at a vacuum pressure of approximately10^{-6} mbar. To fabricate the Pt/MZT/Al memory device, the MZT solution was synthesized as illustrated in the flowchart shown in Fig. 1(a).

The prepared 0.5 M MZT solution was spin-coated on Al electrodes and baked at 100 °C for 15 min. Finally, Pt top electrode of 10^4 μm^2 was sputtered on the MZT thin films to define 1S1R configurations: Pt/MZT/Al/Ni/NbO_2/Ni/PET. The electrical characteristics of all fabricated devices were measured with an Agilent B1500A semiconductor device analyzer.

III. RESULTS AND DISCUSSION

The atomic force microscopy (AFM) image in Fig. 1(b) reveals the surface morphology of the MZT thin film. The root mean square roughness (R_{rms}) of the film was approximately 1.8 nm, indicating the smooth surface of the MZT thin film.

The X-ray photoelectron spectroscopy (XPS) analysis was used to obtain the NbO_2 phase as shown in Fig. 2. Based on the XPS quantitative analysis of the NbO_2 thin film, the atomic percentages of Nb and O were obtained as 34% and 66%, respectively.

The peak for Nb 3d is further examined by high resolution XPS. As displayed in Fig. 3, the Nb 3d spectra of the surfaces (sputter time: <2 min) and inside (sputter time: >3 min) are revealed that the surface of NbO_2 mostly shows Nb^{5+} valence states ($3d_{5/2}$ peak at ∼208 eV and $3d_{3/2}$ peak at ∼210 eV) while the inside of the thin film shows Nb4+ valence state ($3d_{5/2}$ peak at ∼204 eV and $3d_{3/2}$ peak at ∼207 eV), suggesting a qualitative increase of Nb^{5+} and decrease of Nb^{4+} on the surface. This result is similar to [23]. This difference of XPS peaks in surface and inside results from the fact that the Nb^{4+} valence state is unstable and the surface is easily oxidized to be Nb_2O_5 as soon as the NbO_2 films are exposed into the atmosphere [24]. However, due to the injected electrons from the top electrodes will tunnel through the very thin Nb_2O_5 layers by vertical transport, the dominant I-V characteristics of selector device is the NbO_2 layer.

Figure 4(a) shows the threshold-switching properties of the flexible Ni/NbO_2/Ni device. As the applied voltage increased from 0 to 4 V, the current suddenly increased at the threshold voltage ($V_{th,+}$) of 1.6 V, thus changing the electrical property of NbO_2 from the insulating to the metallic state. This corresponds to the onset of the insulator–metal transitions and the device remains in this "on" state as the voltage is increased above the threshold value. By contrast, as the applied voltage decreased from 4 to 0 V, the current suddenly decreased at the hold voltage ($V_{h,+}$) of 0.56 V, thus reverting the electrical property of NbO_2 to the insulating state, referred to as the "off" state. A similar behavior was also observed in negative voltage sweeping, consistent with the nonpolar nature of a thermally induced I-M-T. The threshold

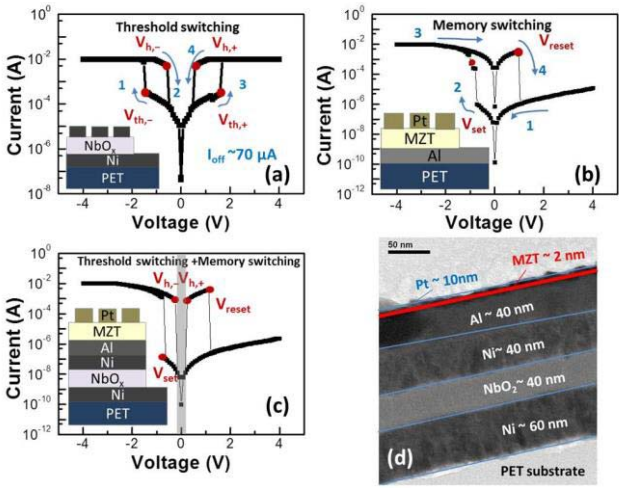

FIGURE 4. ***I–V*** **characteristics and schematic representations of (a) a single Ni/NbO_2/Ni flexible selector, (b) a single Pt/MZT/Al flexible memory device, and(c) 1S1R flexible memory device. (d) TEM image of the proposed 1S1R device structure.**

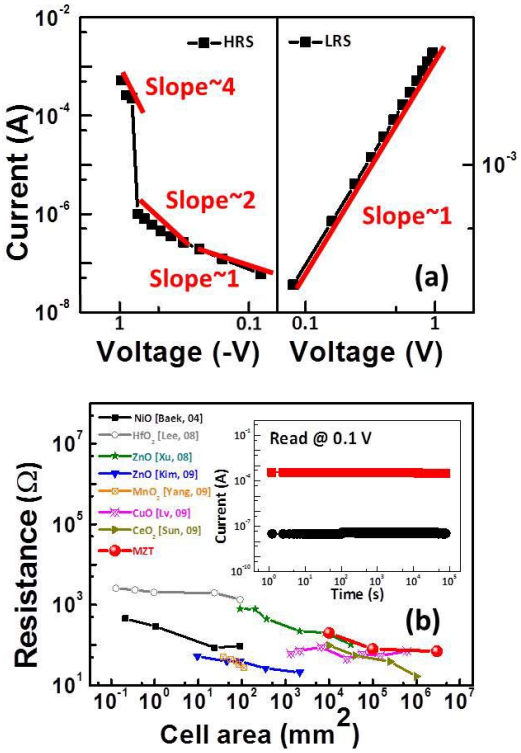

FIGURE 5. **(a) The *log I–log V* curves for the positive voltage regions and the negative voltage regions. (b) LRS resistance versus cell area of various metal–oxide RRAM devices. The inset image shows the retention characteristic of Pt/MZT/Al structure for the LRS and the HRS.**

switching effects in filamentary switching mersisters based on NbO_2 have been attributed to a Joule-heating-induced filamentary insulator-to-metallic phase transformation and shows the "on" and "off" state [17]–[21]. When the current density increases, the temperature of the filament increases and then changes to the metallic phase due to Joule heating.

Figure 4(b) shows the memory-switching properties of the flexible Pt/MZT/Al devices. The devices were reversibly switchable and showed typical bipolar resistive switching behavior. The devices were forming-free because of the sufficient non-lattice oxygen ions in the thin film [25]. A set voltage of -0.96V, a reset voltage of 1V, and an ON/OFF ratio of 10^4 were observed. Merging a threshold-switching Ni/NbO_2/Ni device with a memory-switching Pt/MZT/Al device resulted in a superimposed I–V characteristic, as shown in Fig. 4(c). The gray region of Fig. 4(c) where the current was suppressed. However, compared with [26], the operation current due to the sneak path of the flexible Pt/MZT/Al/Ni/NbO_2/Ni/PET structure is still large and needs further improvements. The continuous read processes, after set or reset, confirmed that these cells exhibit nonvolatile switching behavior with selective properties. The achievable safe margin for the $1/2V_{read}$ scheme depends on the V_{reset} and V_{set} in the memory-switching device and on the Vth and Vh in the threshold-switching device. Thus, the safe margin could be optimized by selecting the appropriate memory and switch materials. Using the NbO_2 selector, the low-resistance state (LRS) current level at the $1/2V_{read}$ approached the near-high resistance state (HRS). By using a resistor in series with the hybrid device with a resistance within the LRS range, the ON/OFF ratio became more controllable. The I-V characteristic at the HRS of 1S1R is lower than that at the HRS of 1S or 1R. Although the I-V characteristics at the LRS of 1S1R is not follow the conductivity of 1S, the LRS current in low-voltage region ($V<V_h$) of 1S1R is lower than the LRS current of 1R. In the view of the fabrication procedures, flexible 1S1R memory device is more complex and has more layers than 1S or 1R device. The more variable factors will affect 1S1R memory device. But the actual reasons behind the reduction of the HRS/LRS current in low-voltage region ($V<V_h$) of 1S1R need to be further investigated. The cross-sectional high-resolution transmission electron microscope (TEM) image of the 1S1R device is shown in Fig. 4(d). The thicknesses of the Ni, NbO_2, Ni, Al, MZT, and Pt layers were approximately 60, 40, 40, 40, 2, and 10 nm, respectively.

To better understand the switching mechanism of the MZT memory device, as can be seen from Fig. 5(a), the logarithmic plots of the I–V curve for the positive and negative voltage sweep regions were plotted. The fitting results in the HRS mode indicate that currents in the negatively biased region typically represent space-charge-limited conduction, which consists of the Ohmic ($I \propto V$) and Child's law regions ($I \propto V^2$) [27]. When all the available traps are filled, the current density abruptly increases with an I–V slope greater than 3 [28]. In the positive voltage region, the current states maintain the LRS and showed ohmic conduction behavior with a slope of around 1, which manifests the formation of conductive filaments [29]. Fig. 5(b) plots the scaling trend of LRS current from the flexible MZT memory device. Due to the switching mechanism of the flexible MZT memory

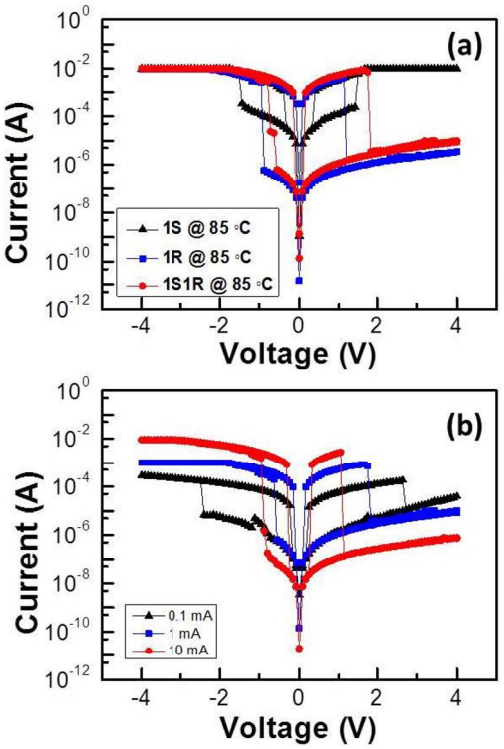

FIGURE 6. ***I–V*** **characteristics of the (a) 1S and 1R, and 1S1R memory devices at 85 °C. (b) The *I-V* curves at low current compliance (I_{cc} < 10 mA).**

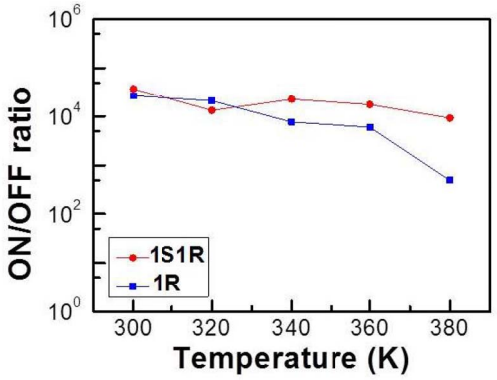

FIGURE 7. ON/OFF ratios of the flexible 1S1R memory devices as a function of temperature from 300 to 380 K.

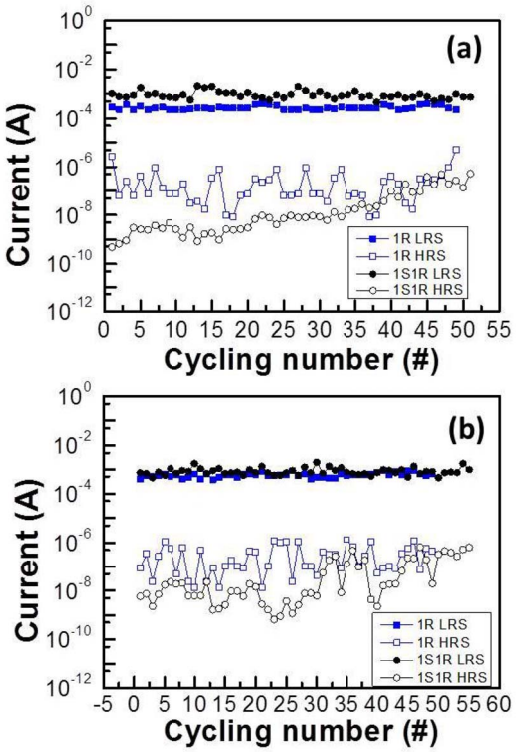

FIGURE 8. Endurance of the flexible 1R and 1S1R memory devices. The V_{set} and $1/2V_{read}$ were (a) 0.5 and (b) 0.25 V.

device was related to the formation and rupture of filaments, the LRS current only has a slight dependence on the cell area. These results are similar to other metal oxides [30], [31]. The inset of Fig. 5(d) shows the retention characteristic at room temperature (RT). The reading voltage was 0.1 V. The ON/OFF ratio of 10^4 and retention ability of over 10^5 s can be achieved by using Pt/MZT/Al structure.

The I–V characteristics of flexible 1S, 1R, and 1S1R memory devices at 85 °C did not noticeably degrade, as shown in Figs. 6(a). Fig. 6(b) shows the I-V curves at low current compliance (Icc<10 mA). When the Icc is below 10 mA, the HRS current has no obvious change, while the LRS current decreases linearly with decreasing Icc and the ON/OFF ratio becomes smaller.

The ON/OFF ratios of the 1R and 1S1R memory device as a function of temperature were measured and are shown in Fig. 7. The ON/OFF ratio of the 1S1R memory device was maintained at 10^4 when the temperature increased to 380 K. The stability of the device at high temperature can be attributed to the suitable I–M–T temperature of NbO_2 for the operation of the flexible 1S1R memory device at 85 °C. Investigating device flexibility is important for practical memory applications.

Fig. 8 shows the endurance properties at a reading voltage of 0.5 V and 0.25V for the flexible 1R and the 1S1R memory devices under DC voltage sweep. The ON/OFF ratio for the flexible MZT memory device is close to 10^2 for the worst case and over 10^3 in general. The ON/OFF ratio for 1S1R memory device can still maintain around 10^4 after 50 consecutive DC measurements. This characteristic is important for flexible memory applications. The degradation of the HRS current might be attributed to the more oxygen-vacancy defects in the filamentary region during I–V cycling [32].

Fig. 9(a) shows the ON/OFF ratios of the flexible 1R and 1S1R memory devices after 400 and 200 bending cycles, respectively. Both the ON/OFF ratios of the flexible 1R and 1S1R memory devices were over 10^4. The 20 mm-long device was bent to a length of 10 mm, even forming a "U"

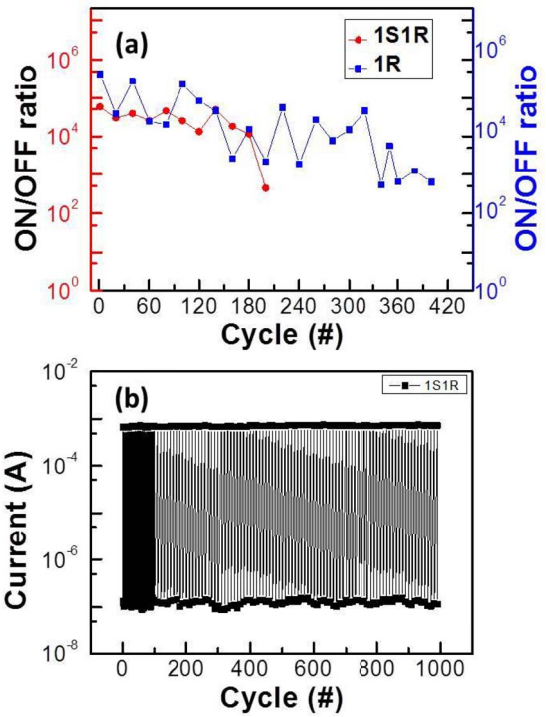

FIGURE 9. (a) DC endurance tests in both HRS and LRS of bending times for 1R and 1S1R devices. (b) Endurance performance of the flexible 1S1R memory devices operated under pulse mode at room temperature (read at 0.5 V).

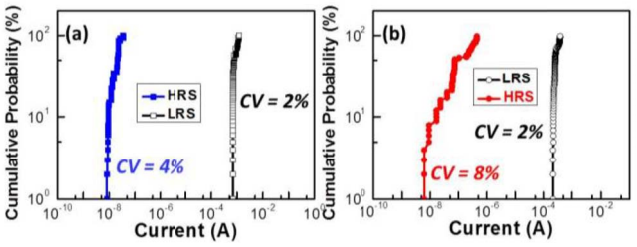

FIGURE 10. Current statistical distributions of the flexible (a) 1R and (b) 1S1R memory devices.

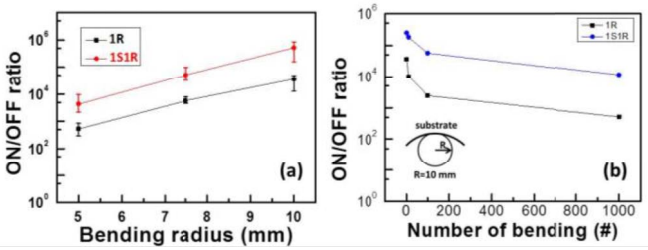

FIGURE 11. (a) The ON/OFF ratio as a function of the bending radius for the 1S1R and 1R memory devices. (b) Continuous bending fatigue test results up to 1000 iterations for the RRAM device.

shape. The ON/OFF ratio of the MZT-based RRAM did not degrade after 300 bending cycles. Moreover, an ON/OFF ratio was distinguishable, signifying the reproducibility and reliability of the flexible RRAM device under mechanical bending stress. In addition, the ON/OFF ratio of the 1S1R memory device after bending 100 cycles maintains over 10^4. These results can be attributed to the smooth MZT thin film, which provide benefits, such as excellent flexibility and electrical stability, to flexible memory applications [33], [34]. The endurance properties of the 1S1R memory devices operated under pulse mode (Programming/Erasing, P/E mode) sweep mode at room temperature are shown in Fig. 9(b). Over 1000 P/E cycle, the variation of the HRS and LRS current is quite stable. Comparison to the DC mode, in general, the endurance performance for the P/E mode is much better than that of DC sweep mode.

Figures 10(a) and (b) present the statistical distribution parameters of the flexible 1R and 1S1R memory devices. Both LRS and HRS currents were measured at 0.5 V. Distribution was evaluated with the coefficient of variation (CV), or the ratio of standard deviation to average value. Both 1R and 1S1R memory devices showed reasonably good separation between LRS and HRS without any overlap, and the fluctuations of the HRS and LRS currents were narrowed. The current CVs for the LRS and the HRS were 2% and 4%, respectively, which are the best data for RRAM devices on flexible substrates. The CVs of the LRS and the HRS currents in the 1S1R memory devices were 2% and 8%, respectively. In general, the broad dispersion of switching parameters in unipolar mode operation is a considerable obstacle in resistive memory applications. Compared with unipolar mode operation [35], [36], the excellent uniformity and reproducibility in the bipolar mode of MZT-based RRAMs are beneficial effects of polarity reversal on limiting oxygen runout. Due to the more complex fabrication procedures, the variation of layer thickness and filament distribution may lead to the wider HRS current distribution of 1S1R memory device than that of 1R memory device. Nevertheless, the 1S1R memory device has relative uniform current distribution and high ON/OFF ratio among other flexible memory devices [37]–[40].

Figure 11(a) shows the ON/OFF ratio as a function of bending radius for the fresh 1R and 1S1R memory devices. For the change of bending radius from 10 to 5 mm, the average ON/OFF ratio of the 1S1R and 1R memory device can still maintain over 10^3 and10^2, respectively. As shown in Fig. 11(b) for the radius of 10mm, the 1S1R and 1R devices also show good mechanical endurance during a bending fatigue test involving 1000 iterations of bending. The ON/OFF ratio retains higher than 10^3 and 10^2, respectively. Compared with that of 1R, better device yield and endurance can be partly attributed to metallic-on and insulating-off states of the 1S1R.

IV. CONCLUSION

A forming-free bipolar resistive switching Pt/MZT/Al device with a threshold-switching Ni/NbO_2 /Ni device on flexible substrate has been demonstrated. The proposed flexible 1S1R

memory device exhibits a good ON/OFF ratio of 10^5 and 10^4 at RT and 85 °C, respectively. This stability can be attributed to the suitable I–M–T temperature of NbO_2 for the operation of flexible 1S1R memory devices at 85 °C. For the change of bending radius from 10 to 5 mm or after bending 10^3 cycles, the ON/OFF ratio of flexible 1S1R memory device can still maintain around 10^3 and 10^5, respectively. The uniform current distribution (CV<10%) in the bipolar mode of flexible 1S1R memory device can be attributed to the good resistive switching behavior of the MZT memory devices. The proposed flexible 1S1R memory devices have potential applications in next-generation nonvolatile memory and flexible electronic equipment.

REFERENCES

[1] Y. Deng *et al.*, "RRAM crossbar array with cell selection device: A device and circuit interaction study," *IEEE Trans. Electron Devices*, vol. 60, no. 2, pp. 719–726, Feb. 2013, doi: 10.1109/TED.2012.2231683.

[2] F. Pan, S. Gao, C. Chen, C. Song, and F. Zeng, "Recent progress in resistive random access memories: Materials, switching mechanisms, and performance," *Mater. Sci. Eng. R Rep.*, vol. 83, pp. 1–59, Sep. 2014, doi: 10.1016/j.mser.2014.06.002.

[3] Y.-C. Chang, K.-J. Lee, C.-J. Lee, L.-W. Wang, and Y.-H. Wang, "Bipolar resistive switching behavior in sol-gel MgTiNiOx memory device," *IEEE J. Electron Devices Soc.*, vol. 4, no. 5, pp. 321–327, Sep. 2016, doi: 10.1109/JEDS.2016.2560879.

[4] K.-J. Lee, Y.-C. Chang, C.-J. Lee, and Y.-H. Wang, "Bipolar and rewritable switching of one diode–one resistor nonvolatile strontium titanate nickelate memory devices," *Vacuum*, vol. 140, pp. 35–41, Jun. 2017, doi: 10.1016/j.vacuum.2016.12.004.

[5] S. Gao *et al.*, "Forming-free and self-rectifying resistive switching of the simple Pt/TaOx/n-Si structure for access device-free high-density memory application," *Nanoscale*, vol. 7, no. 14, pp. 6031–6038, Apr. 2015, doi: 10.1039/C4NR06406B.

[6] S. Gao *et al.*, "Tuning the switching behavior of binary oxide-based resistive memory devices by inserting an ultra-thin chemically active metal nanolayer: A case study on the Ta_2O_5–Ta system," *Phys. Chem. Chem. Phys.*, vol. 17, no. 19, pp. 12849–12856, Apr. 2015, doi: 10.1039/C5CP01235J.

[7] S. Gao *et al.*, "Implementation of complete Boolean logic functions in single complementary resistive switch," *Sci. Rep.*, vol. 5, Oct. 2015, Art. no. 15467, doi: 10.1038/srep15467.

[8] F. A. Chudnovskii, L. L. Odynets, A. L. Pergament, and G. B. Stefanovich, "Electroforming and switching in oxides of transition metals: The role of metal–insulator transition in the switching mechanism," *J. Solid State Chem.*, vol. 122, no. 1, pp. 95–99, Feb. 1996, doi: 10.1006/jssc.1996.0087.

[9] K. Zhang *et al.*, "VO_2-based selection device for passive resistive random access memory application," *IEEE Electron Device Lett.*, vol. 37, no. 8, pp. 978–981, Aug. 2016, doi: 10.1109/LED.2016.2582259.

[10] P.-Y. Chen and S. Yu, "Compact modeling of RRAM devices and its applications in 1T1R and 1S1R array design," *IEEE Trans. Electron Devices*, vol. 62, no. 12, pp. 4022–4028, Dec. 2015, doi: 10.1109/TED.2015.2492421.

[11] H. Pagnia and N. Sotnik, "Bistable switching in electroformed metal–insulator–metal devices," *Physica Status Solidi (A)*, vol. 108, no. 1, pp. 11–65, Jul. 1988, doi: 10.1002/pssa.2211080102.

[12] S. H. Chang *et al.*, "Occurrence of both unipolar memory and threshold resistance switching in a NiO film," *Phys. Rev. Lett.*, vol. 102, no. 2, Jan. 2009, Art. no. 026801, doi: 10.1103/PhysRevLett.102.026801.

[13] M.-J. Lee *et al.*, "Two series oxide resistors applicable to high speed and high density nonvolatile memory," *Adv. Mater.*, vol. 19, no. 22, pp. 3919–3923, Nov. 2007, doi: 10.1002/adma.200700251.

[14] S. Kim *et al.*, "Ultrathin (<10nm) Nb_2O_5/NbO_2 hybrid memory with both memory and selector characteristics for high density 3D vertically stackable RRAM applications," in *Proc. VLSI Technol.*, Honolulu, HI, USA, Jun. 2012, pp. P155–P156, doi: 10.1109/VLSIT.2012.6242508.

[15] M. Zackriya, H. M. Kittur, and A. Chin, "A novel read scheme for large size one-resistor resistive random access memory array," *Sci. Rep.*, vol. 7, Feb. 2017, Art. no. 42375, doi: 10.1038/srep42375.

[16] E. Cha *et al.*, "Nanoscale (~10nm) 3D vertical ReRAM and NbO2 threshold selector with TiN electrode," in *Proc. IEEE Int. Electron Devices Meeting*, Washington, DC, USA, Jan. 2013, pp. 10.5.1–10.5.4, doi: 10.1109/IEDM.2013.6724602.

[17] S. Slesazeck *et al.*, "Physical model of threshold switching in NbO_2 based memristor," *RSC Adv.*, vol. 5, no. 124, pp. 102318–102322, Nov. 2015, doi: 10.1039/C5RA19300A.

[18] C. Funck *et al.*, "Multidimensional simulation of threshold switching in NbO_2 based on an electric field triggered thermal runaway model," *Adv. Electron. Mater.*, vol. 2, no. 7, Jul. 2016, Art. no. 1600169, doi: 10.1002/aelm.201600169.

[19] J. Kim, C. Ko, A. Frenzel, S. Ramanathan, and J. E. Hoffman, "Nanoscale imaging and control of resistance switching in VO_2 at room temperature," *Appl. Phys. Lett.*, vol. 96, no. 21, May 2010, Art. no. 213106, doi: 10.1063/1.3435466.

[20] M. D. Pickett, J. Borghetti, J. J. Yang, G. Medeiros-Ribeiro, and R. S. Williams, "Coexistence of memristance and negative differential resistance in a nanoscale metal-oxide-metal system," *Adv. Mater.*, vol. 23, no. 15, pp. 1730–1733, Apr. 2011, doi: 10.1002/adma.201004497.

[21] M. D. Pickett and R. S. Williams, "Sub-100 fJ and sub-nanosecond thermally driven threshold switching in niobium oxide crosspoint nanodevices," *Nanotechnology*, vol. 23, no. 21, Jun. 2012, Art. no. 215202, doi: 10.1088/0957-4484/23/21/215202.

[22] F. Mouraa *et al.*, "Dielectric and ferroelectric characteristics of barium zirconate titanate ceramics prepared from mixed oxide method," *J. Alloys Compounds*, vol. 462, nos. 1–2, pp. 129–134, Aug. 2008. doi: 10.1016/j.jallcom.2007.07.077.

[23] M. Kang, S. Yu, and J. Son, "Voltage-induced insulator-to-metal transition of hydrogen-treated NbO_2 thin films," *J. Phys. D Appl. Phys.*, vol. 48, no. 9, Feb. 2015, Art. no. 095301, doi: 10.1088/0022-3727/48/9/095301.

[24] F. J. Wong, N. Hong, and S. Ramanathan, "Orbital splitting and optical conductivity of the insulating state of NbO_2," *Phys. Rev. B, Condens. Matter*, vol. 90, Sep. 2014, Art. no. 115135, doi: 10.1103/PhysRevB.90.115135.

[25] A. Kim, K. Song, Y. Kim, and J. Moon, "All solution-processed, fully transparent resistive memory devices," *ACS Appl. Mater. Interfaces*, vol. 3, pp. 4525–4530, Oct. 2011, doi: 10.1021/am201215e.

[26] P. Huang *et al.*, "Self-selection RRAM cell with sub-μA switching current and robust reliability fabricated by high-K/metal gate CMOS compatible technology," *IEEE Trans. Electron Devices*, vol. 63, no. 11, pp. 4295–4301, Nov. 2016, doi: 10.1109/TED.2016.2612824.

[27] M. A. Lampert, "Simplified theory of space-charge-limited currents in an insulator with traps," *Phys. Rev.*, vol. 103, pp. 1648–1656, Sep. 1956, doi: 10.1103/PhysRev.103.1648.

[28] Y.-C. Chang, R.-Y. Xue, and Y.-H. Wang, "Multilayered barium titanate thin films by sol-gel method for nonvolatile memory application," *IEEE Trans. Electron Devices*, vol. 61, no. 12, pp. 4090–4097, Dec. 2014, doi: 10.1109/TED.2014.2363651.

[29] Z. S. Wang *et al.*, "Reproducible and controllable organic resistive memory based on Al/poly(3,4-ethylene-dioxythiophene): poly(styrenesulfonate)/Al structure," *Appl. Phys. Lett.*, vol. 97, no. 25, Dec. 2010, Art. no. 253301, doi: 10.1063/1.3529455.

[30] H.-S. P. Wong *et al.*, "Metal–oxide RRAM," *Proc. IEEE*, vol. 100, no. 6, pp. 1951–1970, Jun. 2012, doi: 10.1109/JPROC.2012.2190369.

[31] K.-J. Lee, L.-W. Wang, T.-K. Chiang, and Y.-H. Wang, "Effects of electrodes on the switching behavior of strontium titanate nickelate resistive random access memory," *Materials*, vol. 8, no. 10, pp. 7191–7198, 2015, doi: 10.3390/ma8105374.

[32] L. Goux *et al.*, "Evidences of oxygen-mediated resistive-switching mechanism in Tin\HfO2\Pt cells," *Appl. Phys. Lett.*, vol. 97, no. 24, Dec. 2010, Art. no. 243509, doi: 10.1063/1.3527086.

[33] Y.-H. Hwang, H.-M. An, and W.-J. Cho, "Performance improvement of the resistive memory properties of InGaZnO thin films by using microwave irradiation," *Jpn. J. Appl. Phys.*, vol. 53, Feb. 2014, Art. no. 04EJ04, doi: 10.7567/JJAP.53.04EJ04.

[34] K.-J. Lee *et al.*, "Sol-gel strontium titanate nickelate thin films for flexible nonvolatile memory applications," *IEEE Trans. Electron Devices*, vol. 64, no. 5, pp. 2001–2007, May 2017, doi: 10.1109/TED.2016.2637925.

[35] K. Jung *et al.*, "Unipolar resistive switching in insulating niobium oxide film and probing electroforming induced metallic components," *J. Appl. Phys.*, vol. 109, no. 5, Mar. 2011, Art. no. 054511, doi: 10.1063/1.3552980.
[36] K. Jung *et al.*, "Electrically induced conducting nanochannels in an amorphous resistive switching niobium oxide film," *Appl. Phys. Lett.*, vol. 97, no. 23, Dec. 2010, Art. no. 233509, doi: 10.1063/1.3525710.
[37] Z. Q. Wang *et al.*, "Flexible resistive switching memory device based on amorphous InGaZnO film with excellent mechanical endurance," *IEEE Electron Device Lett.*, vol. 32, no. 10, pp. 1442–1444, Oct. 2011, doi: 10.1109/LED.2011.2162311.
[38] K. I. Chou, C. H. Cheng, Z. W. Zheng, M. Liu, and A. Chin, "Ni/GeOx/TiOy/TaN RRAM on flexible substrate with excellent resistance distribution," *IEEE Electron Device Lett.*, vol. 34, no. 4, pp. 505–507, Apr. 2013, doi: 10.1109/LED.2013.2243814.
[39] C.-C. Lin, H.-Y. Wu, N.-C. Lin, and C.-H. Lin, "Graphene-oxide-based resistive switching device for flexible nonvolatile memory application," *Jpn. J. Appl. Phys.*, vol. 53, Mar. 2014, Art. no. 05FD03, doi: 10.7567/JJAP.53.05FD03.
[40] C.-H. Cheng, F.-S. Yeh, and A. Chin, "Low-power high-performance non-volatile memory on a flexible substrate with excellent endurance," *Adv. Mater.*, vol. 23, no. 7, pp. 902–905, 2010, doi: 10.1002/adma.201002946.

KE-JING LEE was born in Tainan, Taiwan. She received the B.S. degree from the Department of Electronic Engineering, Kao Yuan University, Kaohsiung, Taiwan, in 2006 and the M.S. degree from the Department of Electro-Optical Engineering, Southern Taiwan University of Science and Technology, Tainan, in 2008. She is currently pursuing the Ph.D. degree with the Institute of Microelectronics, National Cheng-Kung University, Tainan. Her research focused on organic transistors and memory devices with solution-processed insulators.

YU-CHI CHANG was born in Chiayi, Taiwan. She received the B.S. degree from the Department of Applied Physics, National Kaohsiung University, Kaohsiung, Taiwan, in 2011 and the Ph.D. degree from the Institute of Microelectronics, National Cheng-Kung University, Tainan, Taiwan, in 2015. Her research focused on organic transistors and memory devices with solution-processed insulators.

CHENG-JUNG LEE was born in Taichung, Taiwan. He received the B.S. degree from the Department of Electronic Engineering, Nan Jeon University of Science and Technology, Tainan, Taiwan, in 2007 and the M.S. degree from the Department of Electro-Optical Engineering, Kun Shan University, Tainan, in 2012. He is currently pursuing the Ph.D. degree with the Institute of Microelectronics, National Cheng-Kung University, Tainan. His research focused on organic transistors with solution-processed insulators.

LI-WEN WANG was born in Tainan, Taiwan. She received the B.S. degree from the Department of Electrical Engineering, National Kaohsiung University, Kaohsiung, Taiwan, in 2016. She is currently pursuing the M.S. degree with the Department of Electrical Engineering, National Cheng-Kung University. Her researches focused on solution-processed high-permittivity insulators for organic transistors, resistive random-access memory devices applications.

YEONG-HER WANG (M'89) was born in Tainan, Taiwan. He received the B.S. and Ph.D. degrees in electrical engineering from National Cheng-Kung University, Taiwan, in 1978 and 1985, respectively. He is currently a Distinguished Professor with the Institute of Microelectronics, Department of Electrical Engineering, National Cheng-Kung University. He has published over 370 refereed journal papers, 110 Taiwan patents, and 23 U.S. patents. His research activities are on semiconductor devices, MMIC design and fabrication.